The formation of the ettringite from sulfate solutions

H.Y.Ghorab[1], A.M.Zayed[2] ,A.S.Mohamed[1], M.R.Mabrouk[1],
[1]*Helwan University, Cairo Egypt,* [2] *University of South Florida, USA*

The ettringite phase was obtained from lime and aluminum sulfate solutions with variable sulfate concentrations at room temperature. Three series were investigated; the first with a sulfate amount equal to the stoichiometry of the ettringite, the second and third were sulfate-deficient with gibbsite phase in the mixture. The mole ratio S'/A* was kept constant at 3, 2 and 1 in the three series respectively. Increasing concentrations of lime suspensions were added to the sulfate or sulfate/gibbsite mixtures with a starting mole ratio of C/S'=1 to 2, 3, 6 and end value of C/A = 6. The solids obtained after two minutes stirring were identified. The composition of the filtrates was determined. The results indicate the formation of ettringite with different sulfate concentrations. It appears as needle and fiber-like particles. The mechanism of formation is discussed.

1. Introduction

The composition of the natural mineral ettringite is $Ca_6Al_2(SO_4)_3(OH)_{12}.26H_2O$. It has a needle shape with columns composed of $[Ca_6[Al(OH)_6]_2.24H_2O]^{6+}$ and channels in which the $[(SO_4)_3.\sim 2H_2O]^{6-}$ are located [1]. The hydroxyl ions unite the calcium and aluminum polyhedra into a chain and are responsible for the column's bond strength. Water does not take part in binding the columns but joins them into a single crystal. The positive charge is distributed among the water molecules and the negative among SO_4^{2-} tetrahedron where every group interacts with the surface of more than one column to balance the charge. At room temperature, whenever aluminum and sulfate ions are available, the ettringite forms with the supply of lime at pH values of 11-13. The minimum concentrations of the sulfate needed for its formation was reported to be 2mg SO_3 [2]. Its stability is attributed to the markedly low solubility product further lowered in lime solutions [3-5]. The conditions of its formation are satisfied in many systems. In cement it is formed through the reaction of C_3A and C_4AF with calcium- and alkali sulfate phases [6]. It is obtained from the reaction of aluminum sulfate with lime in aqueous solutions, of aluminum hydroxide, slag or metakaolin with lime and gypsum and through the hydration of the calcium sulfoaluminate [7-11]. Its morphology varies from colloidal to needle-like particles of variable length depending on the conditions of formation [8]. Very thin crystals were obtained from calcium sulfate solutions of low concentrations in the presence of calcium aluminate, the size of the crystals increased upon standing.

---

*The following abbreviations are used in this paper: CaO=C, SO_3=S', Al_2O_3=A

The mechanism of its formation is solid-solid, topochemical or through solution. Hardened cement systems with ettringite are susceptible to expansion in sulfate solutions. In the present paper, the ettringite is prepared through the reaction of lime with aluminum sulfate solutions of variable sulfate concentrations, also in the presence of gibbsite, at room temperature. The mechanisms of its formation are discussed.

2. Experimental

The materials used were chemically pure calcium hydroxide, hydrated aluminium sulfate, gama aluminium hydroxide (gibbsite) and distilled water [12]. The preparation of ettringite refers to the reaction of calcium hydroxide with aluminium sulfate in aqueous solution at room temperature according to Equation (1). The mole ratio of S'/A is equal to 3, C/S'= 2 and C/A = 6.

$$6CaO + Al_2(SO_4)_3.8H_2O + H_2O \longrightarrow 6CaO.Al_2O_3.3SO_3.32H_2O \quad (1).$$

Three series of investigation were carried out. In the first the aluminum sulfate salt was weighed in 250 ml solution to provide an amount of sulfate equivalent to a mole ratio of S'/A =3 which satisfies the stoichiometry of the ettringite. In the second and third series the weights of aluminum sulfate corresponded to mole ratios of S'/A =2 and 1; gibbsite was added to the sulfate solutions to maintain the desired ratio. 250 ml of lime suspensions with increasing lime contents were rapidly added to each of the sulfate or the sulfate gibbsite mixtures in 11 separate steps. The starting mole ratio of lime to sulfate was C/S'=1 and ended with values of C/S'=2, 3, 6 in the three series respectively. An end ratio of C/A =6 was kept in the three series. Table (1) shows the weights of reactants used.

Table (1): The weights of reactants used to prepare ettringite

First series S'/A=3 AS'_3H_{18}=26.65g , AH_3=-			Second series S'/A=2 AS'_3H_{18}=17.79g ,AH_3=2.08g-			Third series S'/A=1 AS'_3H_{18}=8.88 , AH_3=4.16g		
C/S\	C/A	Lime (g/l)	C/S\	C/A	lime (g/l)	C/S\	C/A	lime (g/l)
1.0	3.0	8.8908	1.0	2.0	5.9272	1.0	1.0	2.9636
1.1	3.3	9.7798	1.2	2.4	7.1126	1.5	1.5	4.4454
1.2	3.6	10.6689	1.4	2.8	8.2981	2.0	2.0	5.9272
1.3	3.9	11.5580	1.6	3.2	9.4835	2.5	2.5	7.4090
1.4	4.2	12.4471	1.8	3.6	10.6690	3.0	3.0	8.8908
1.5	4.5	13.3362	2.0	4.0	11.8544	3.5	3.5	10/3726
1.6	4.8	14.2252	2.2	4.4	13.0398	4.0	4.0	11.8544
1.7	5.1	15.1143	2.4	4.8	14.2253	4.5	4.5	13.3362
1.8	5.4	16.0034/	2.6	5.2	15.4107	5.0	5.0	14.8180
1.9	5.7	16.8925	2.8	5.6	16.5962	5.5	5.5	16.2998
2.0	6.0	17.7816	3.0	6.0	17.7816	6.0	6.0	17.7816

The mixtures were stirred for two minutes then filtered off quickly. The filtrates were slightly acidified then analyzed gravimetrically to determine the dissolved sulfate and volumetrically to estimate the concentrations of aluminum and calcium in solutions [13]. The solids were dried 1day at 50^{o}C and characterized by means of X-ray diffraction .Their morphology was examined on Hitachi scanning electron microscope type S-3400N with EDAX attachment type. Their oxide composition and free lime content were determined wet chemically [14]. Table (2) illustrates the empirical formulae of the solids collected in the different series based on the analyses of lime, sulfate and alumina of the solids.

Table (2): The empirical formulae of the solids obtained from the different series.

First series S'/A=3		**Second series S'/A=2**		**Third series S'/A=1**	
$C_xAS\backslash_z$	**C/S**	**$C_xAS\backslash_z$**	**C/S**	**$C_xAS\backslash_z$**	**C/S**
$C_{1.69}AS\backslash_{1.94}$	0.87	$C_{0.85}AS\backslash_{1.15}$	0.73	$C_{0.38}AS\backslash_{0.44}$	0.80
$C_{1.92}AS\backslash_{1.96}$	0.96	$C_{1.14}AS\backslash_{1.00}$	1.14	$C_{0.64}AS\backslash_{0.43}$	1.48
$C_{2.01}AS\backslash_{1.83}$	1.09	$C_{1.37}AS\backslash_{1.00}$	1.37	$C_{0.92}AS\backslash_{0.44}$	2.13
$C_{2.09}AS\backslash_{1.71}$	1.09	$C_{1.64}AS\backslash_{1.00}$	1.64	$C_{1.22}AS\backslash_{0.44}$	2.77
$C_{2.07}AS\backslash_{1.57}$	1.31	$C_{1.87}AS\backslash_{1.04}$	1.79	$C_{1.36}AS\backslash_{0.45}$	3.02
$C_{2.23}AS\backslash_{1.59}$	1.40	$C_{2.14}AS\backslash_{1.04}$	2.05	$C_{1.58}AS\backslash_{0.47}$	3.36
$C_{2.37}AS\backslash_{1.56}$	1.51	$C_{2.33}AS\backslash_{1.01}$	2.30	$C_{1.85}AS\backslash_{0.47}$	3.93
$C_{2.66}AS\backslash_{1.58}$	1.68	$C_{2.61}AS\backslash_{1.02}$	2.55	$C_{2.07}AS\backslash_{0.47}$	4.40
$C_{2.84}AS\backslash_{1.58}$	1.79	$C_{2.67}AS\backslash_{1.07}$	2.49	$C_{2.39}AS\backslash_{0.47}$	5.08
$C_{2.70}AS\backslash_{1.47}$	1.83	$C_{3.02}AS\backslash_{1.08}$	2.79	$C_{2.57}AS\backslash_{0.49}$	5.24
$C_{2.92}AS\backslash_{1.47}$	1.98	$C_{3.17}AS\backslash_{1.08}$	2.93	$C_{3.01}AS\backslash_{0.49}$	6.14

3. Results

The change in the solution composition of the series studied is plotted as a function of lime addition expressed as C/S' ratio. In the solubility curves, the dissolved ions are denoted by gSO_4^{2-}/l, gAl/l and gCaO/l for sulfate, aluminum and lime. The solubility curves are illustrated beside the variation in the free lime content of the solids with lime addition in Figures 1, 3 and 5 for the three series respectively. In the same figures, the X-ray diffraction patterns of representative solids collected from the series are shown. Figures 2, 4 and 6 show the morphology and EDAX analysis of three chosen solids E_3, E_2 and E_1collected from the three series.

3.1. First Series: The ettringite formation from S'/A=3, maximum ratios of C/S'=2 and of C/A=6

Figure 1 illustrates that at the first lime addition of C/S'=1 in the investigation series (S'/A=3), the concentration of the dissolved sulfate amounts to 1.0gSO_4^{2-}/l. It shows an insignificant decrease until a C/S'=1.3, followed by a rapid and sharp depletion to C/S'=1.4 (0.69gSO_4^{2-}/). It slows down to

C/S'=1.6 at which ratio an extremely weak and diffused depression is observed. At further lime additions it changes only slightly and at C/S'=1.8-1.9 it undergoes a second depletion after which a constant value of 0.4g SO_4^{2-}/l is maintained. A related behavior is observed in the aluminum of the solution which starts with a value of 0.6gAl/l at C/S'=1. It decreases first gradually then noticeably at C/S'=1.3-1.4. With further lime additions it remains constant then undergoes a sharp and clear depletion at ~C/S'=1.8 up to an almost complete consumption. The dissolved lime does not change significantly until C/S'=1.6 where it decreases sharply then remains constant with a value of 0.58gCaO/l.

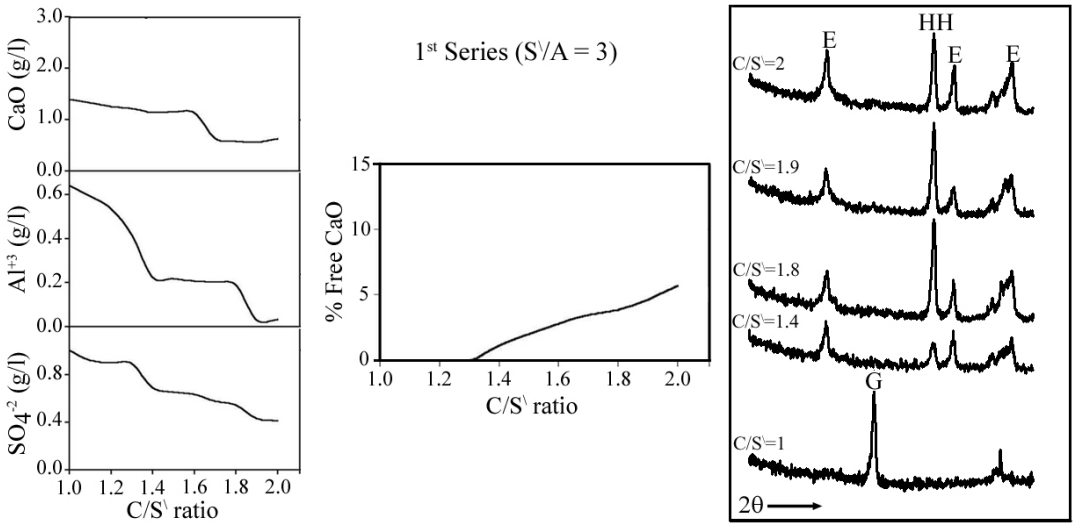

Figure 1: The variation of the solution composition and the free lime content as a function of lime addition in the first series (S'/A=3), also the X-ray diffractograms of some chosen solids of the series.

The free lime is monitored first in the solid collected at C/S'=1.3 and its percentage rises steadily to 5.68% at C/S'=2. It is clear from the X-ray diffractograms of Figure (1) that gypsum is the only hydrate detected up to a C/S'=1. Weak ettringite patterns were detected simultaneous to the appearance of the free lime in the solid at C/S'=1.3 and well defined lines are recognized in the specimen collected at C/S'=1.4 (Fig.1). The ettringite formation also matches with the depletion of the dissolved sulfate and aluminum from the solution at C/S'=1.3-1.4 without a noticeable change in the dissolved lime. This means that the free portlandite residing in the solid reacts with the solution in favor of the formation of the calcium sulfoaluminate hydrate phase. Gypsum disappears with the appearance of the ettringite at C/S'=1.3 which indicates its consumption in the sulfoaluminate phase. The characteristic lines of the ettringite was seen to weaken and became more diffuse with further lime addition of C/S'=1.5 to

1.7 i.e. throughout the constancy observed of the aluminum concentration of the solution. In this C/S' range the hemihydrate precipitated probably as a result of the reaction of the dissolved lime - indicated by it depletion at C/S'=1.6 - with the sulfate ions showing a weak depression at ~ C/S'=1.6. Sharp ettringite patterns, however, reappear at C/S'=1.8 matching with the second depletion stage of the dissolved sulfate and aluminum from the solution. Again, the unvaried concentration of the dissolved lime indicates the role of portlandite as the solid reactant which interacts with the dissolved ions leading to the precipitation of well crystallized ettringite. At the stoichiometric ratio of the ettringite (C/S'=2), the following phases exist in the solid: Well crystallized ettringite, hemihydrate, 5.68% portlandite which might carbonate upon standing to calcite. These phases are present in an aluminum free solution with low sulfate and calcium ion concentrations. The morphology of the solid E_3 collected at the first appearance of free lime (C/S'=1.3) illustrates the existence of the well known ettringite needle (Fig. 2). The particles are ~ 2 microns long and ~0.6micron wide. They are surrounded by shapeless gel particulates. The EDAX attachment shows a calcium to sulfur to aluminum ratio fitting the stoichiometric formula CaO: SO_3: Al_2O_3 = 6:3:1.

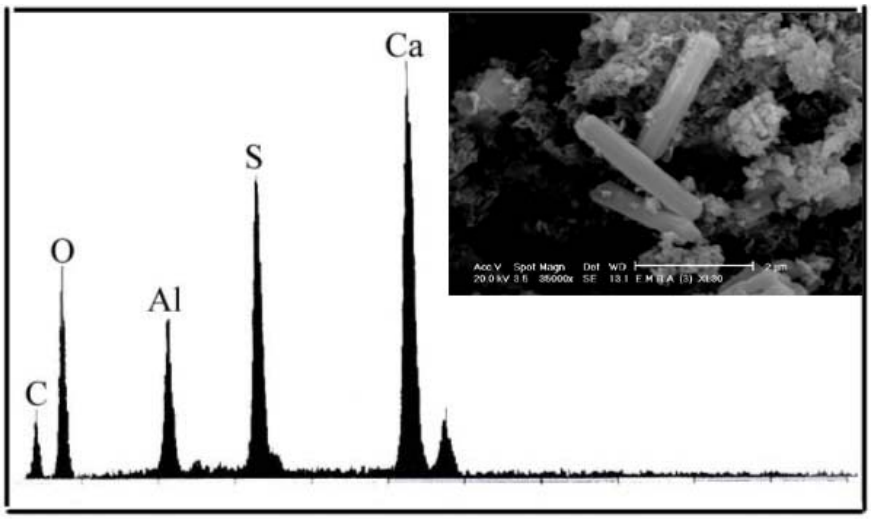

Figure 2: The morphology of the ettringite appearing as needles in the E_3 solid obtained from the first series with S'/A=3 at C/S'=1.4. The EDAX indicates a sulfate concentration fitting to the stoichiometric value of the ettringite

3.2. Second series: The ettringite formation from S'/A=2, maximum ratios of C/S'=3 and C/A=6

In the second investigation series with S'/A=2, the sulfate ion concentration of the solution is equal to 0.8g SO_4^{2-}/l at C/S'=1. It remains more or less constant with lime addition up to C/S'=1.6 (Fig. 3). In the range of C/S'= 1.6-

2 it is depleted to 0.64g SO_4^{2-}/l. A second depletion stage is seen at C/S'=2.2- 2.6 after which a solubility value of 0.33g SO_4^{2-}/l is reached and remains constant. The aluminium concentration of the solution is low and shows a steady value of 0.23 gAl/l over the range studied. A very weak depression is, however, detected at C/S'=2-2.5. The dissolved lime indicates a gradual decrease with increasing the C/S' ratio. It passes through a minimum of 0.15gCaO/l at C/S'=2.4 then rises again in the solution to attain a solubility of ~0.97 CaO/l at C/S'=3. The free lime appears in the solids at C/S'=1.6 at which ratio the ettringite phase is detected as shown in the X-ray diffractogram of Fig. (3). The ettringite formation occurs simultaneous to a parallel consumption of gibbsite indicated from the weakening of its d-value line at 4.88A. This occurs parallel to the depletion of the dissolved sulfate at a C/S'=1.6.

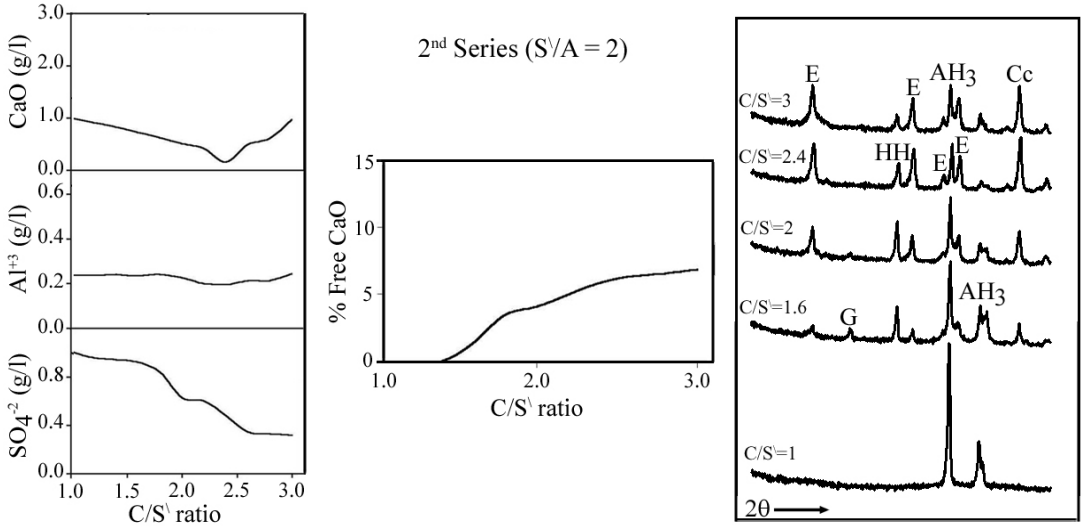

Figure 3: The variation of the solution composition and the free lime content as a function of lime addition in the second series with S'/A=2, also the X-ray diffractograms of some chosen solids of the series.

As in the first series, the weakly varied concentration of lime in the solution indicates the reaction of portlandite with gibbsite and the dissolved sulfate. At the C/S'=2 the d-value lines of the ettringite sharpen indicating its crystallization. At C/S'=2-2.5 the crystallization of ettringite is accompanied by another weakening of gibbsite, a minimum value of the dissolved lime and a further depletion of sulfate. In other words, the portlandite reacts further with gibbsite and with the dissolved sulfate and an extra consumption of lime from the solution to form well crystallized ettringite. At C/S'=3 the following phases exist in the solid: Ettringite, hemihydrate, a little amount of gibbsite and portlandite susceptible to carbonation. The solution is poor in sulfate and aluminum and rich in calcium. The ettringite in the E_2 solid

appears as thin needle few hundred nanometers in length and width. It is embedded in a gel matrix and was detected with difficulty (Fig. 4). In the same figure, the EDAX attachment shows sulfur content less than the stoichiometric ratio.

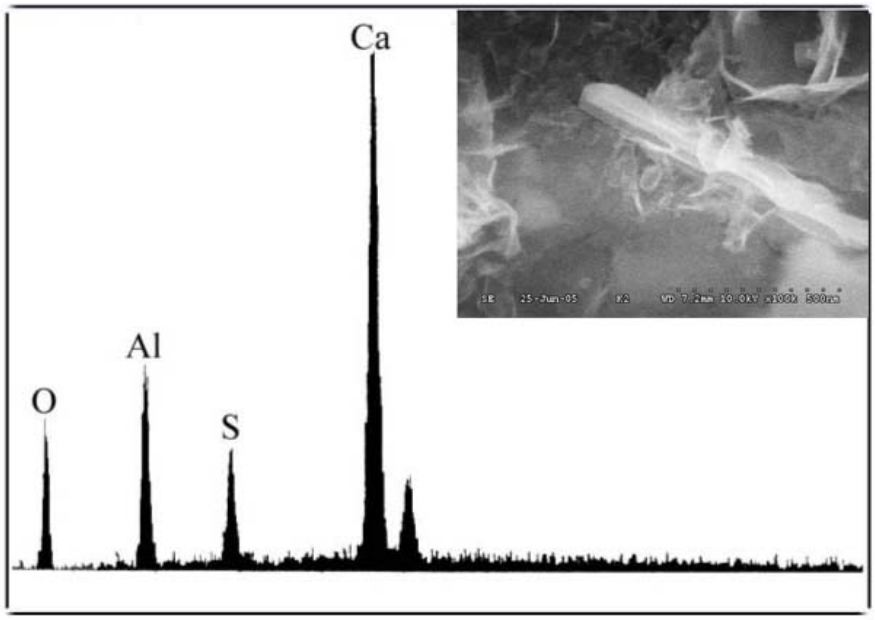

Figure 4: The morphology of the ettringite appearing as thin needles in the E_2 solid obtained from the second series with S'/A=2 at C/S'=1.6. The EDAX indicates a sulfate concentration lower than the stoichiometric value of the ettringite

3.3. The third series: The ettringite formation from S'/A=1, maximum ratios of C/S'=6 and C/A=6

The sulfate ion concentration of the third series with S'/A=1 is equal to 0.8g SO_4^{2-}/l at C/S'=1. It undergoes a relatively smooth depression with lime addition. At C/S'= 2 it slows down to a constant value of 0.37 gSO_4^{2-}/l. In this diffused curve a very weak depression is recognized at C/S'=2-2.5. Similar to the second series, the aluminium concentration of the solution shows a more or less constant value of ~0.23gAl/l over the range studied, a very weak depletion is, however, observed at C/S'=2.5. The dissolved lime decreases gradually from 0.76.gCaO/l to a minimum value of 0.6gCaO/l at C/S'=2.5 then rises to 1.4 gCaO/l at C/S'=6. The free lime appears in this series at C/S'=2.5 with a value of 0.48%. It increases only slightly with higher lime addition until C/S'= 4.5 then rises up to 13.8% at C/S'=6. This retardation in the increase of free lime suggests its active consumption in the solid. In this series, well defined ettringite patterns appear first at C/S'=2 and remain until 2.5. The ettringite formation takes place with the consumption of part of gibbsite indicated by the weakening of the 4.38A line with a simultaneous very weak consumption of the dissolved aluminum and a

diffused depletion of the sulfate from the solution at a minimum concentration of dissolved lime. The hemihydrate appears beside the ettringite. In the range of C/S'=2.5 to 4.5 and parallel to the insignificant variation of the free lime in the solids, the d-value lines of the ettringite weaken and the patterns become more diffused. This occurs without the contribution of the liquid phase since the sulfate and aluminium are constant with low values and the solution is lime-rich. At the further release of the free lime from the solid at C/S'=5, the monophases form and the hemihydrate vanishes. At C/S'=5-6 the following phases exist in the solids: Ettringite, monophases, gibbsite and portlandite susceptible to carbonation. They exist in contact with a solution poor in aluminum and sulfate, rich in calcium. The ettringite detected in the E_1 solid is a fiber- like agglomerate of a nanometer scale. Similar to that of the E_2 solid its sulfur content is lower than the stoichiometric (Fig. 6).

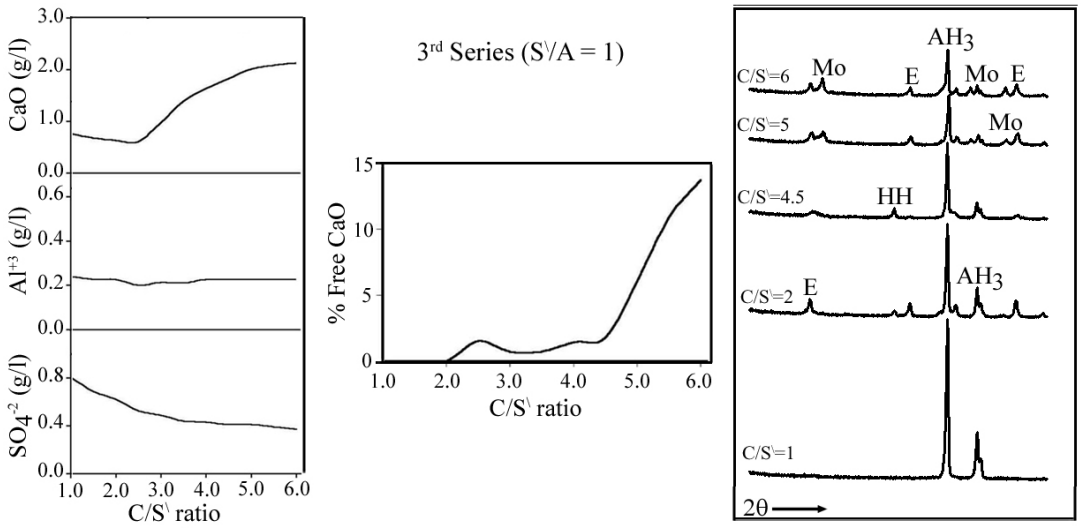

Figure 5: The variation of the solution composition and the free lime content as a function of lime addition in the third series with S'/A=1, also the X-ray diffractograms of some chosen solids of the series.

4. Discussion

The formation of ettringite from the reaction of lime added to aluminum sulfate solutions of different sulfate concentrations, also in the presence of gibbsite at room temperature occurs in two stages. The first takes place as soon as the free lime appears in the solid after the termination of the process of its combination with the available reactants. The present investigation indicates the combination of lime with sulfate to form gypsum which patterns weaken with decreasing the S'/A ratios. At the first appearance of free lime in the solids it reacts with the dissolved sulfate, incorporates the calcium sulfate phases formed at lower C/S' ratios and consumes the available aluminum present either in solution and./or provided as gibbsite to form

ettringite, the dissolved lime plays little role in this process and only portlandite acts.

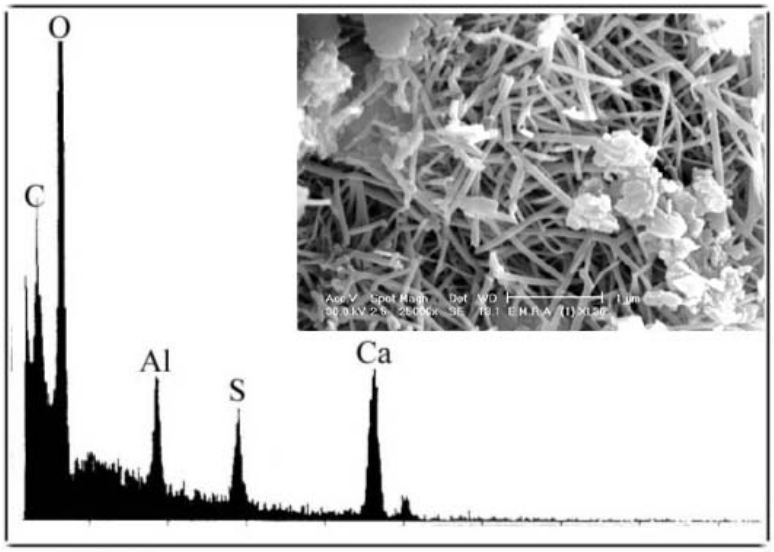

Figure 6: The morphology of the ettringite appearing as fiber-like particles in the E_1 solid obtained from the third series with S'/A=1 at C/S'=2.0. The EDAX indicates a sulfate concentration lower than the stoichiometric value of the ettringite

The second stage of the ettringite formation is found at the stoichiometric value of the C/S'=2 which ratio seems to have a significant meaning in its crystallization from sulfate solutions. At this ratio, the ettringite formation is accompanied by the incorporation of the remaining sulfate, aluminate and lime from the solution and includes also the consumption of gibbsite and portlandite from the solid. The ettringite formed is well crystallized. In the mixtures of S'/A=3 and 2, C/S'=2, 3 and C/A=6, it exists with hemihydrate, portlandite and gibbsite if added as reactant. In the third series with S'/A=1 the ettringite phase survives lime addition of C/S'=4.5 then converts partly to the monosulfate hydrate with a further consumption of gibbsite. Both calcium sulfoaluminate phases reside with gibbsite and portlandite in a lime rich solution, poor of aluminum and sulfate. The amount of sulfate in this solid is originally equivalent to an S'/A=1 and distributes itself between both types of calcium sulfoaluminate hydrates. The ettringite phase present is sulfate-deficient. The monophases incorporate portlandite in their structure as seen from the low free lime content up to C/S'=4.5. In other words, the appearance of the monophases and the partly conversion of ettringite to the monosulfate hydrate occur at enough lime supply, in the presence of aluminum hydroxide in the solid (gibbsite) and sulfate poor systems.. Further work is needed to define the distribution of sulfate in these multiphase solids also to follow up the change in the morphology of the ettringite in the different solutions. The different morphology of the ettringite phase varying

from needle to fiber-like appearance and indicates its strong dependence on the sulfate content incorporated in its structure. The ettringite patterns detected after its first appearance weaken and become more diffuse with increasing the lime concentration in the solution which predicts the increase of its colloidal character and a further reduction in the crystallite size. This occurs at a dormant period of the aluminate clearly observed in the first series in which the dissolved aluminum remains constant in solution. It is also indicated by the constancy of the gibbsite patterns in the solids collected from the second and third series after the first appearance of the ettringite. The dormant period of the aluminate and the aluminum-bearing phase deserves to be noted.

5. Conclusion

Two mechanisms are detected for the formation of the ettringite from the reaction of lime with aluminum sulfate solution with variable sulfate concentrations, also in the presence of gibbsite. The first occurs at C/S'< 2 as soon as the free lime appears in the solid and the second at the stoichiometric ratio C/S'= 2. The conversion of the ettringite to the monosulfate hydrate occurs in sulfate deficient medium of S'/A=1 at C/S'=5 through the consumption of portlandite, gibbsite and hemihydrate, in a solution poor in sulfate and aluminum, rich in lime. Both types of the calcium sulfoaluminate hydrate phases persist together with portlandite and gibbsite. The results indicate the incorporation of variable sulfate concentration in the structure of the ettringite. Its morphology varies from needle to fiber-like with lowering the sulfate content in the solid.

6. References

[1] H. F. W. Taylor and A. E. Moore, Nature 218 (1968) 1048.

[2] J. D'Ans, H. Eick, Zement Kalk Gips 6 (1953) 302.

[3] H. Y. Ghorab, E. A. Kishar, Studies on the Stability of the Calcium Sulfoaluminate Hydrate. Part 1: The Stability of Ettringite in Pure Water, Cement and Concrete Research 15 (1985) 93-99

[4] E.A. Kishar, Kinetic Studies on the Stability of Some Calcium Aluminate Hydrate, M.Sc. Thesis, 1986. Studies on the Stabilities of Hydration Products of Portland Cement, Ph.D. Thesis, 1991.

[5] C.J. Warren, E.J. Reardon, The solubility of ettringite at 25°C, Cement and Concrete Research, 24 (1994)1515.

[6] H.E. Schwiete, U. Ludwig, P.Jaeger, Investigations in the System $3CaO-Al_2O_3-CaSO_4-CaO-H_2O$, Symposium on Structure of Portland Cement Paste and Concrete, Highway Research Board, Special Report 90 (1966) 353

[7] Y. Shimada, J.F. Young, Thermal stability of ettringite in alkaline solutions at 80°C, Cement and Concrete Research 34 (2004) 2261

[8] F. W. Lerch, R.H. Bogue, F.W. Ashton, The Sulfoaluminates of Calcium, Journal of Research of the National Bureau of Standards 2 (1929) 715
[9] Lea's Chemistry of cement and concrete Fourth edition 1998.pp 459.
[10] P. K. Mehta, Mechanism of expansion associated with ettringite formation, Cement and Concrete Research 3 (1) (1973)
[11] F.P. Glasser, Advances in sulfoaluminate cements, The 5th International Symposium on Cement and Concrete Shanghai, China (1) (2002). 14-25.
[12] A.S. Mohamed, Studies on the expansion behavior of ettringite in pure systems and in cement pastes, M. Sc. Thesis Helwan University Cairo Egypt, 2006
[13] Vogel, A Text Book of Quantitative Inorganic Analysis, Longmans, Green &Co. White Planes, New York, 1961
[14] N. A. Gabr, Steam curing of slag cement, Ph. D. Thesis, Ain Shams University, Cairo, Egypt, 1978

Acknowledgement
The authors would like to express their appreciation to Eng. Helmut Brandt, Hitachi High technologies, Krefeld Germany for his valuable assistance in studying the morphology of the ettringite –bearing solids.